Hindawi
Mathematical Problems in Engineering
Volume 2022, Article ID 7754356, 16 pages
https://doi.org/10.1155/2022/7754356

Research Article

Insulation Resistance Measurement of Airport Navigational Lighting System Based on Deep Learning and Transfer Learning

Z. B. Liu,[1] **Q. Wang**,[2] **H. Li**,[2] **C. Y. Wang**,[2] **and J. Y. Fei**[2]

[1]*School of Mechanical Engineering, Dalian Jiaotong University, Dalian 116028, China*
[2]*School of Locomotive and Rolling Stock Engineering, Dalian Jiaotong University, Dalian 116028, China*

Correspondence should be addressed to J. Y. Fei; fjy@djtu.edu.cn

Received 25 July 2022; Accepted 6 September 2022; Published 25 September 2022

Academic Editor: Chao Huang

The insulation resistance value is one of the important indexes for the safe operation of airport navigational lighting system. In this paper, a method based on deep learning and transfer learning is proposed to measure the insulation resistance value. To reduce the influence of high voltage environment and signal injection on the measurement accuracy, a multilayer LSTM model is established, in which the network convergence rate is accelerated by introducing a normalized layer in front of the first LSTM layer. Based on the constructed deep network, transfer learning is employed by sharing the weight parameters of the pretraining model to solve the problem of small data sample. The experimental results demonstrate that the proposed method can effectively improve the measurement accuracy of the insulation resistance value.

1. Introduction

The airport navigational lighting system (ANLS) is necessary visual navigation that aids to ensure the safe take-off and landing of the aircraft in special circumstances [1–3]. In the lighting system, almost all the lights are installed outdoors, and the power supply cables are mostly buried in the field. Due to the environmental factors such as ground temperature, humidity, and mold, the phenomenon of water branches is caused, which makes the cables insulation worse [4–7]. If not handled on time, it will cause a short circuit between the cable core and the ground, resulting in a light bulb failure among the grounding points, which will threaten the safety of aircraft take-off and landing to varying degrees. Thus, the working status of the ANLS can be judged by the insulation resistance value of the ANLS circuit cable.

General airport lighting stations are equipped with 500 V and 2500 V hand shaking megohm meter. 500 V is used for periodic inspection of insulate on resistance of low voltage electrical equipment or insulation fault detection, and 2500 V is mainly used for periodic inspection of insulation resistance of light circuit or insulation fault detection. All of these require manual testing, which cannot guarantee personal safety, and there are cases of untimely fault detection. This leads to intelligent insulation resistance testing technology.

The existing insulation measurement technology is typically classified into balance bridge method and signal injection method [8–11]. The basic principle of measuring insulation resistance with balanced bridge method is to connect two individual resistors with DC high voltage line under the Earth ground and use resistors and switches to form a bridge to obtain the differential current loops and corresponding voltages, thereby converting the insulation resistance value. Papers [12, 13] adopt the balanced bridge method, which have a similar application method. It mainly checks the resistance between the positive and negative DC bus and the ground equivalent potential node to determine the insulation state. These methods require electronic switches or high voltage relays and current or voltage sensors. With the advantages of simple measurement, the method still exist some deficiencies. The most notable defects are low sensitivity, reliability, and mechanical wear caused by mechanical switch relays, as well as the lack of consistency and accuracy of the circuit caused by the multiple operational amplifiers. Moreover, the resistance

can only be measured without current. Online measurement will not only cause measurement misalignment but also damage the measuring instrument or even endanger personal safety if the voltage of the measured line is higher than the test high voltage of the instrument. Therefore, this method is not suitable for online monitoring. The basic principle of measuring insulation resistance by signal injection method is to inject a voltage signal of a certain frequency between the insulated cable and the ground and calculate the insulation resistance by measuring the feedback signal. Paper [14] establishes a series battery pack model composed of first-order resistor-capacitance (RC) circuit cell units. Based on this series battery pack model, the insulation monitoring model of low voltage and low frequency signal injection method is designed. The insulation monitoring method in paper [15] is based on the measurement of the differential current of each power supply line. When the insulation resistance is reduced, the leakage current flows to ground, and the differential current in the line can be measured to prevent the occurrence of faults. Paper [16] proposes a method to dynamically change the reference measurement resistance according to the DC bus voltage. This method uses an intermediate value as the reference resistance prediction test value and dynamically changes the reference resistance value according to this prediction value to obtain the test result of insulation resistance. However, the accuracy of insulation resistance measured by these methods is limited by high voltage, interference, and other factors, and it is difficult to determine the selection of injected signals in the signal injection method. Moreover, the ripple of the DC system will be increased, which will affect the quality of power supply and sampling accuracy.

Deep learning has been widely applied in some fields with the in-depth development. In recent years, it has also been applied in circuits. Aiming at the problems of low accuracy and weak robustness of traditional fault line selection method for small current grounding system, a new method based on improved GoogLeNet was proposed in paper [17]. In this paper, the zero-sequence current signal is mapped to a two-dimensional time-frequency diagram by wavelet transform, and the small current grounding data set is prepared. Then, the fault line selection of the small current grounding system is carried out by using the GoogLeNet model. In paper [18], deep learning is applied to diagnose the interturn short circuit problem for permanent magnet synchronous motors. An efficient and accurate method based on a conditional generative adversarial net and an optimized sparse auto encoder is proposed to detect the interturn short circuit problem for permanent magnet synchronous motors. The experimental results indicate that the fault diagnosis accuracy achieves 98.9%. The successful application of deep learning in circuits shows the practicability and applicability of deep learning in the field of circuits. Therefore, a method of the insulation resistance value is proposed based on deep learning and transfer learning. Finally, the experimental measurement results demonstrate that this method can measure the insulation resistance value effectively and the relative error with the calibration value is controlled within 0.6%. Moreover, three different insulation resistance measurement methods are compared in this paper, including switching time-sharing method, deep learning without transfer learning method, as well as the deep learning and transfer learning method proposed in this paper. Compared with the traditional switching time-sharing method, the results show that the measurement accuracy of the deep learning method is greatly improved. At the same time, compared with the measurement method using deep learning alone, the measurement accuracy of insulation resistance value is improved by at least 1% based on the deep learning and transfer learning method proposed in this paper. It can be concluded from the data that the insulation resistance value calculation method based on deep learning and transfer learning proposed in this paper can effectively improve the detection effect of the insulation resistance value cable.

The main contributions of this paper are summarized as follows:

(1) Transfer learning is applied for the first time to solve the problem of small sample size of insulation resistance measurement under high voltage by sharing the pretraining model weight

(2) A multilayer LSTM model is built to minimize the impact of the high voltage environment and injected voltage signal on the insulation resistance measurement accuracy

The remainder of this article is set out as follows. Section 2 introduces the structure of the ANLS and the method for measuring the basic value of insulation resistance. Then, the measurement error of insulation resistance is analyzed. In Section 3, the idea of deep learning and transfer learning method proposed in this paper is described, which mainly analyzes the acquisition of source domain data and the construction of the source domain model. After comparing the effects of the LSTM model and GRU model in this method, the multilayer LSTM model architecture is finally selected. In Section 4, the experimental setup and results are also introduced and this section carries on the comparative experiment and the analysis of the three measurement methods. Finally, Section 5 draws the conclusion and the outlook.

2. Insulation Resistance Measurement Structure of ANLS and Error Analysis

2.1. Structure of ANLS. ANLS is composed of low voltage power distribution system (including substation, standby diesel generator set, relay protection, and switching device), constant current dimmer (including booster transformer), cables, and lamps distributed on the runway of the airport (including isolation transformers and bulbs) [19, 20]. A schematic diagram of a circuit in the ANLS is shown in Figure 1. In order to avoid the impact of single bulb damage on the power supply of the whole circuit, the bulbs in the ANLS are connected in series 1 : 1 through the isolating

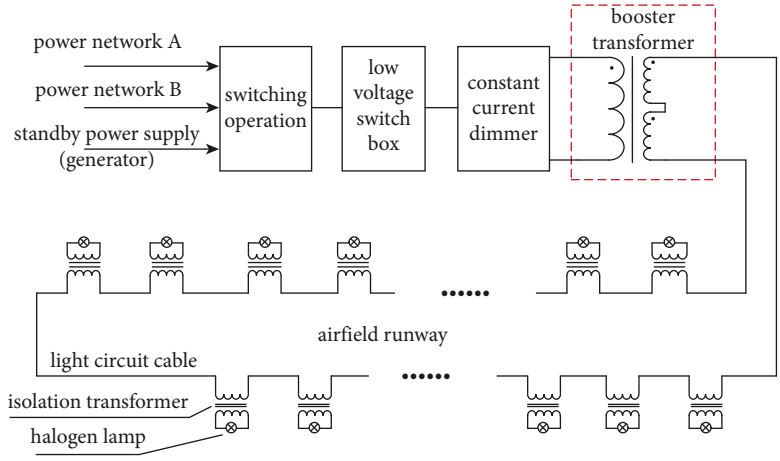

Figure 1: A circuit of the ANLS.

transformer in light circuit cable [21–23]. The constant current dimmer adjusts the effective value of the output voltage according to the change of the load size so that the current in the load loop remains constant at the light level that meets the set brightness level.

2.2. Insulation Resistance Basic Value Acquisition. Based on the switching time-sharing detection method proposed by the author Zhang in previous papers [24], the basic value of insulation resistance was obtained. This method not only reduces the influence of alternating current on measurement but also reduces the influence of cable water tree effect on measurement results. The better deep network model can be trained by using higher precision raw data.

As shown in Figure 2, the insulation resistance detection device has two terminals. The "*a*" terminal connected with the current sampling resistor R_I is directly grounded and the "*b*" terminal connected with the current limiting protection resistor R_0 is connected to the cable in the ANLS circuit. The resistance value R_X of the insulation resistance based on the switching time-sharing detection method is calculated as shown in the following equation:

$$R_X = \frac{U_d}{(I_{d+a} - I_a)} - R_0 - R_I. \tag{1}$$

Then, R_X is taken as the basic measurement value of cable insulation resistance for subsequent processing.

In Figure 2, U_d is the 24 V low voltage DC precision power supply, R_0 is the current limiting protection resistor with a resistance value of 1MΩ, R_I is the current sampling resistor with a resistance value of 1 kΩ, C_I is the filter capacitor, KF is the relay, R_X is the unknown equivalent insulation resistor, and U_a is the unknown equivalent AC voltage source.

2.3. Error Analysis of Cable Insulation Resistance Measurement. 30 kVA constant current dimmer is taken as an example. When the dimmer is turned on, considering the worst case of the measuring circuit (refers to the highest voltage under which the AC working voltage is 100% added

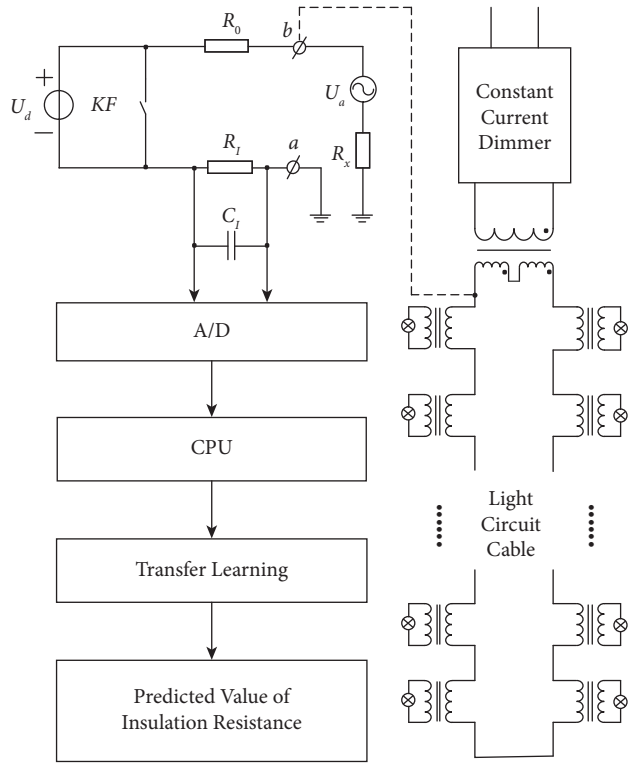

Figure 2: Real-time monitoring structure of insulation resistance.

to the insulation resistance), the maximum effective value of the output AC voltage is 4545 V. According to the circuit theory, when the insulation resistance is in the normal range, R_0 and R_I can be ignored, and then the maximum voltage that the insulation resistance R_X bears is as follows:

$$V_{\max} = U_d + 1.1 \times \sqrt{2} \times 4545V. \tag{2}$$

When the ANLS is running, it is assumed that the stray external interference current is I_g. As shown in Figure 2, the current flowing through the insulation resistance in the ideal state is shown in equation (3) and in the case of interference is shown in equation (4).

$$I_R = I_0, \tag{3}$$

$$I_R' = I_0 + I_g. \tag{4}$$

At this point, the absolute error of insulation resistance measurement is as follows:

$$D = R_x' - R_x = \frac{U_d}{\left(I_0 + I_g\right)} - \frac{U_d}{I_0}. \tag{5}$$

The relative error is as follows:

$$D_R = \left|\frac{D}{R_x'}\right| \times 100\% = \left|\frac{R_x'}{R_x - 1}\right| \times 100\% = \left|\frac{1}{I_0/I_g + 1}\right| \times 100\%. \tag{6}$$

According to equation (6), the greater the interference current I_g is, the greater the relative error D_R is. In order to enhance the anti-interference ability, the existing means mostly use 500 V or higher excitation power U_d. When the cable is selected, the insulation resistance R_X is certain. Only when the value of U_d is larger, I_0 will be larger correspondingly, the influence of the interference current I_g on the error will be relatively small, and the anti-interference ability will increase accordingly. However, the voltage sustained by the insulated cable at this time is at least 500 V higher than that without the installation of online detection device, which increases the electric field strength sustained by the insulated cable. The injection of large voltage signal in the detection circuit leads to the breakdown and leakage of the cable instead of the normal working circuit, which shortens the service life of the cable. Therefore, some scholars began to reduce the injection voltage in order to reduce the influence of electric field intensity. However, with the decrease of the injection voltage, the relative error of the system measurement increases. The selection of the injection signal threshold has not been clearly explained, and whether the injection of the signal will affect the measurement results of the insulation resistance value is not known.

At the same time, the stray current I_g cannot be determined and the interference current generated by AC alone and the interference current generated by AC and DC together cannot be determined to be the same value numerically, so the interference caused by stray current cannot be eliminated simply through the difference method. The aging degree of insulated cables caused by external environment cannot be deduced by precise mathematical formula.

Based on the above discussion, this paper proposes a method to measure the insulation resistance value based on deep learning and transfer learning. The LSTM model is used to train the relationship between the input and output of cable insulation resistance under low voltage condition, and the weight parameters are shared with the model under high voltage condition through transfer learning so as to improve the measurement accuracy of the model. The normalization layer is introduced in front of the first LSTM layer to accelerate the convergence rate of the network.

3. Insulation Resistance Measurement Based on Deep Learning and Transfer Learning

3.1. Overall Structure. This paper proposes a method of insulation resistance measurement for the ANLS circuit cable based on deep learning and transfer learning; the technical process is shown in Figure 3.

The specific operation steps are as follows:

Step 1. When the constant current dimmer is turned off, the standard resistance with known resistance value R_{ys} is used to simulate the working condition of the AMLS circuit cable insulation resistance under low voltage. Then, the basic measurement value of the resistance R_{xs} is measured by switching time-sharing method.

Step 2. A multilayer LSTM network framework is constructed, and R_{xs} is taken as the input value and R_{ys} as the output value and the network convergence speed is accelerated by introducing a normalized layer in front of the first LSTM layer. Then, it is trained and denoted as Net_s, and the network was evaluated.

Step 3. When the constant current dimmer is turned on, the standard resistance with known resistance value R_{yt} is parallel with the circuit cable, and the change of the insulation resistance value of the cable in the ANLS is simulated. Then, the basic measurement value of the resistance R_{xt} is measured by switching time-sharing method.

Step 4. The input layer and the LSTM hidden layer of Net_s are kept, that is, the weight parameters of Net_s network are kept, and the full connection layer and the output layer of Net_s are rebuilt. The normalization layer is also added to accelerate the convergence rate.

Step 5. R_{xt} is taken as the input value and R_{yt} as the output value. Then, it is trained and denoted as Net_t, and the network is evaluated.

Step 6. The insulation resistance value is measured using Net_t.

3.2. Source Domain Data Acquisition. Firstly, the source domain data of insulation resistance are measured under low voltage working environment. When there is a fault in the system, the specific performance is that the insulation resistance value changes. Therefore, a precision resistance A with known resistance value is made in parallel in the circuit, as shown in Figure 4. By closing the miniature toggle switch, a series of resistors with different resistance values can be obtained to simulate the insulation resistance of the cable. Connect resistor A to the "Target Plate" as shown in Figure 5.

Place the device at room temperature and turn on the power. Then, turn on the switch of resistor A in Figure 4 and measure according to the steps in Section 2.2 to obtain a set of data. After cooling off the power and the equipment, measurements are made again after turning on the power and repeated for 6 times to form source domain data $\{R_{xs}, R_{ys}\}_1, \{R_{xs}, R_{ys}\}_2, \ldots, \{R_{xs}, R_{ys}\}_6$. The six sets of sequence data are divided into training set and test set according to 4 : 2.

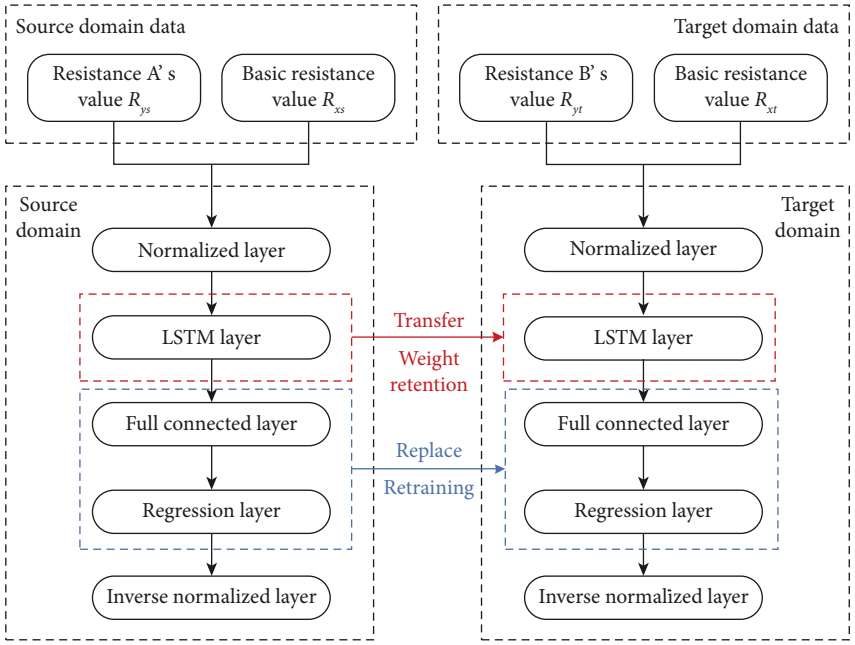

Figure 3: Technical process.

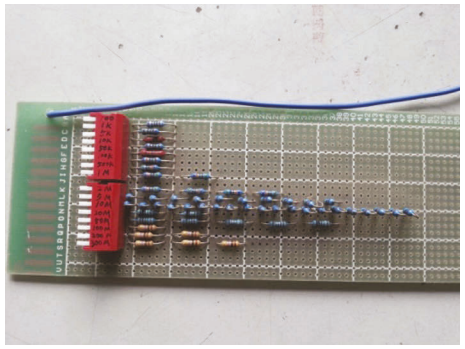

Figure 4: The standard resistance A.

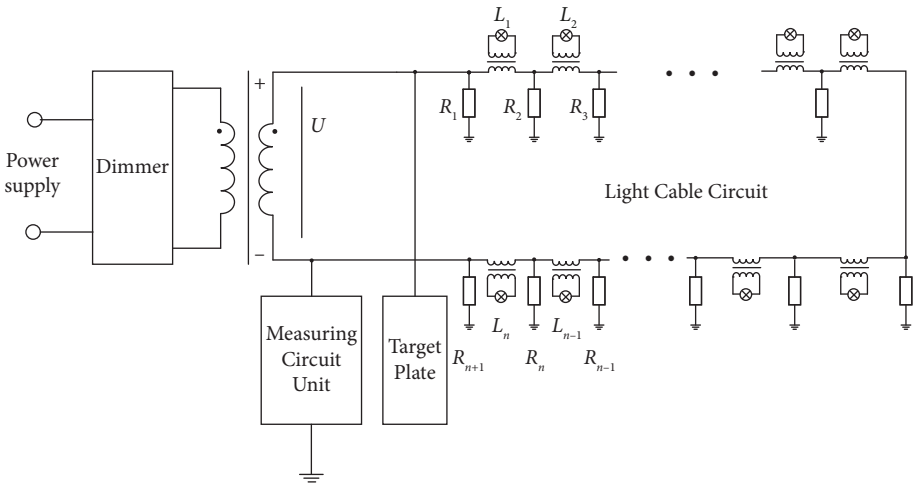

Figure 5: Wiring method of the experimental device.

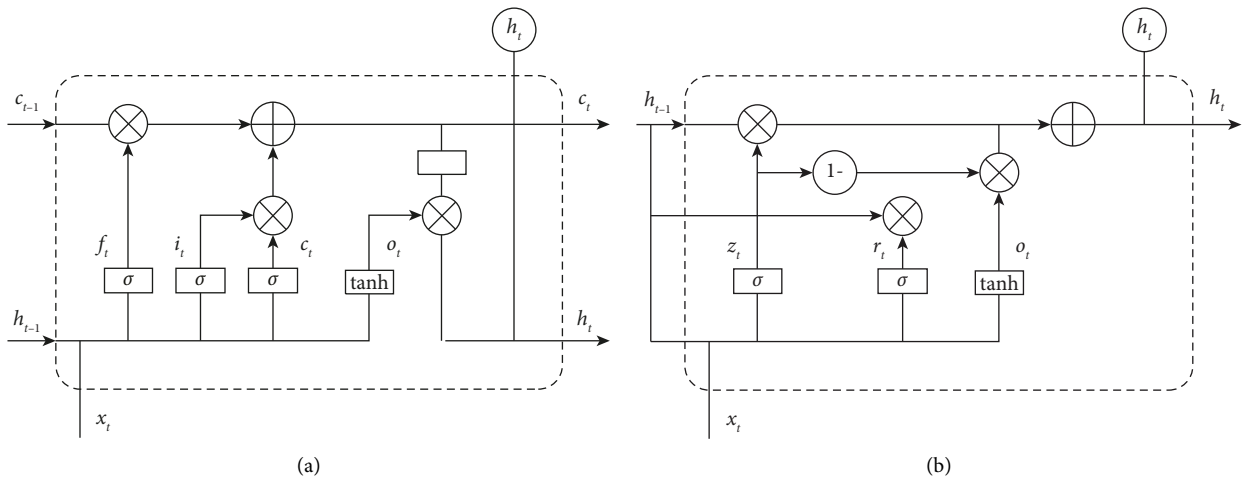

Figure 6: LSTM and GRU unit structure. (a) LSTM. (b) GRU.

3.3. Multilayer LSTM Network Construction and Performance Analysis. With the rise of artificial intelligence, some deep learning models have been proposed specifically for data prediction problems, such as the long short-term memory (LSTM) network and gate recurrent unit (GRU) network. The LSTM network was first proposed by Hochreiter and Schmidhuber in 1997. LSTM network is designed to solve the long-term dependence problem of deep learning, which is improved by recurrent neural network (RNN) [25, 26]. Now, it is widely used in the fields of text generation, speech recognition, and image generation description [27]. The GRU network is a type of recurrent neural network (RNN) [28, 29]. It is also proposed to solve the problems of long-term memory and gradients in back propagation, just like the LSTM. The internal network structure of LSTM and GRU is basically the same, and the biggest difference is shown as follows: LSTM network structure takes output gate o_t, input gate i_t, and forget gate f_t as the internal state, while GRU combines the latter two into update gate z_t, deletes the output gate, and adds reset gate r_t, which takes update and reset gate as the internal state. The details of the unit structure for both are shown in Figure 6.

These two deep learning models are substituted into the method of this paper, which is used to train the relationship between the input and output of cable insulation resistance of the source domain to reduce the influence of high voltage environment and signal injection on the measurement accuracy.

3.3.1. LSTM Network. Firstly, the LSTM network is brought in, and in order to accelerate the convergence rate of the model, a normalized layer is added in front of the first LSTM layer. The structural design is shown in Figure 7.

The LSTM model designed in Figure 7 is used as the pretraining model. Among them, there are 200 hidden layers, 1000 times of training, and the learning rate is 0.001. The training effect is shown in Figure 8. The pretraining network is evaluated, and the prediction effect of the test set was shown in Figures 9–11.

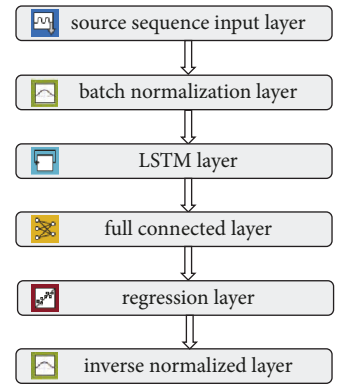

Figure 7: Source domain training model based on LSTM.

Figure 9 shows the measurement results of insulation resistance values corresponding to the two test sets. The error of the measured value compared with the real value and the corresponding relative error are shown in Figures 10 and 11. As can be seen from Figures 9–11, the effect of the pretraining model is effective, and the relative error of the insulation resistance value obtained on the test set can be controlled within 2.4%.

3.3.2. GRU Network. Similar to the method based on the LSTM network, a multilayer GRU model is also established, and a normalization layer is added to accelerate the convergence speed of the model. 200 hidden layers were set in the GRU network and trained for 1000 times, the learning rate was set to 0.001. The training effect is shown in Figure 12. The pretraining network is evaluated, and the prediction effect of the test set is shown in Figures 13–15.

Figure 13 shows the measurement results of insulation resistance values corresponding to the two test sets. The error of the measured value compared with the real value and the corresponding relative error are shown in Figures 14 and 15.

As can be seen from Figures 14 and 15, the relative error of the insulation resistance value obtained on the test set of

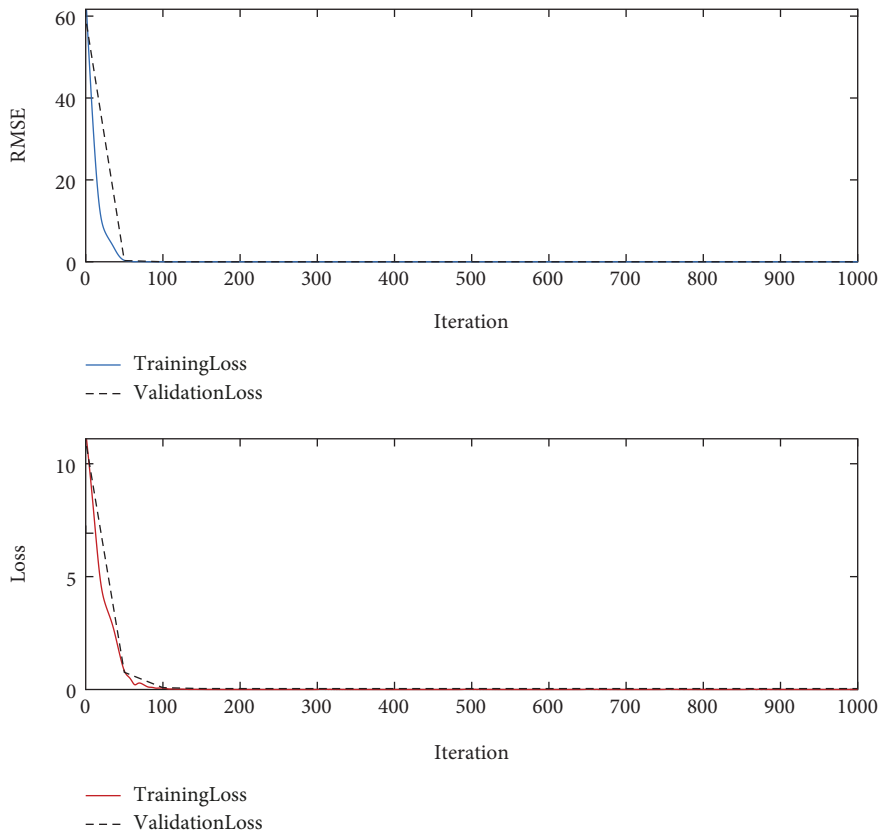

Figure 8: Pretraining effect of the source domain model by LSTM.

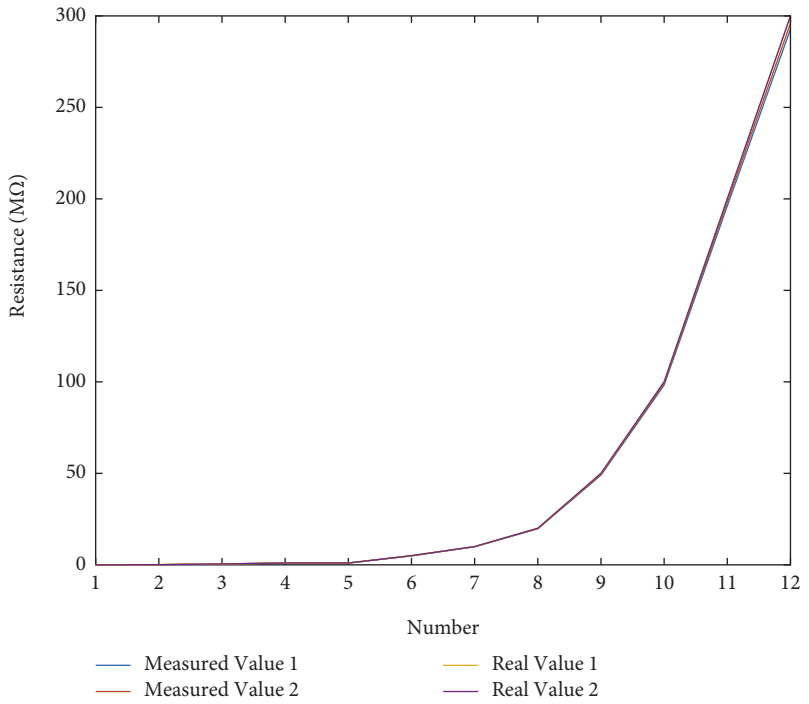

Figure 9: Measured values of insulation resistance.

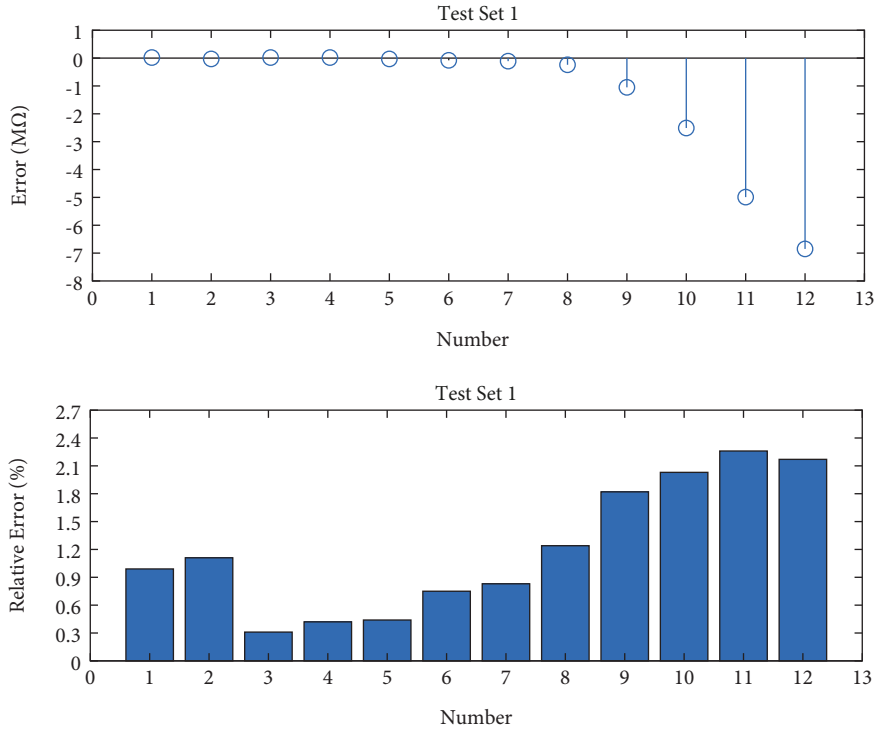

Figure 10: Diagram of insulation resistance measurement error and relative error in test set 1.

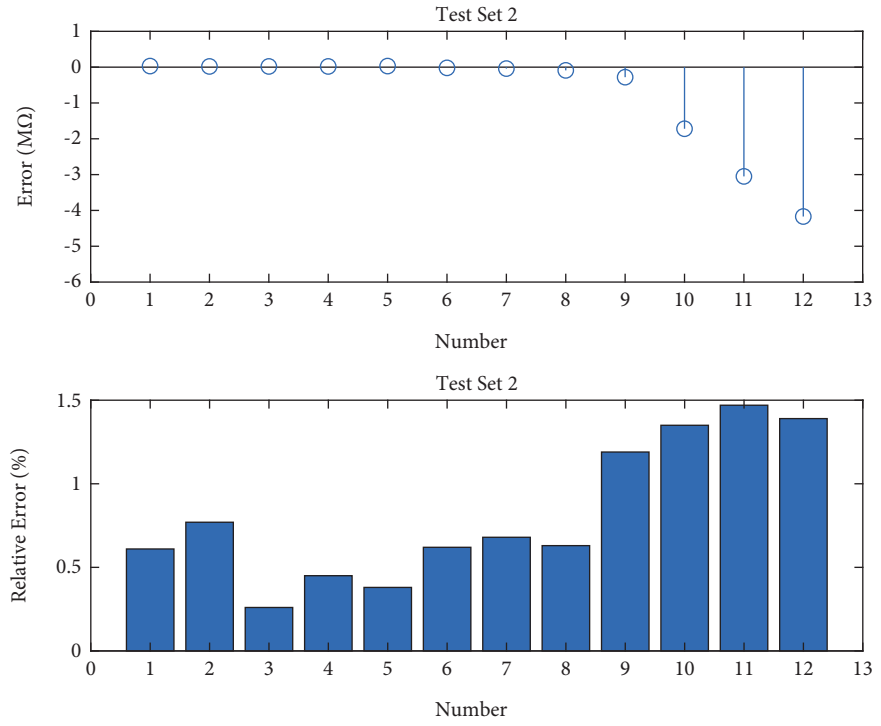

Figure 11: Diagram of insulation resistance measurement error and relative error in test set 2.

the model trained by GRU network is controlled within 3.5%. Compared with the LSTM model, it can be seen that the precision of insulation resistance measurement results of GUR network fluctuates greatly. Although the relative error is small in the section with low insulation resistance value, the relative error increases suddenly in the section with high insulation resistance value and the measurement effect is unstable. Therefore, a multilayer LSTM model is selected as the basic network architecture in this paper.

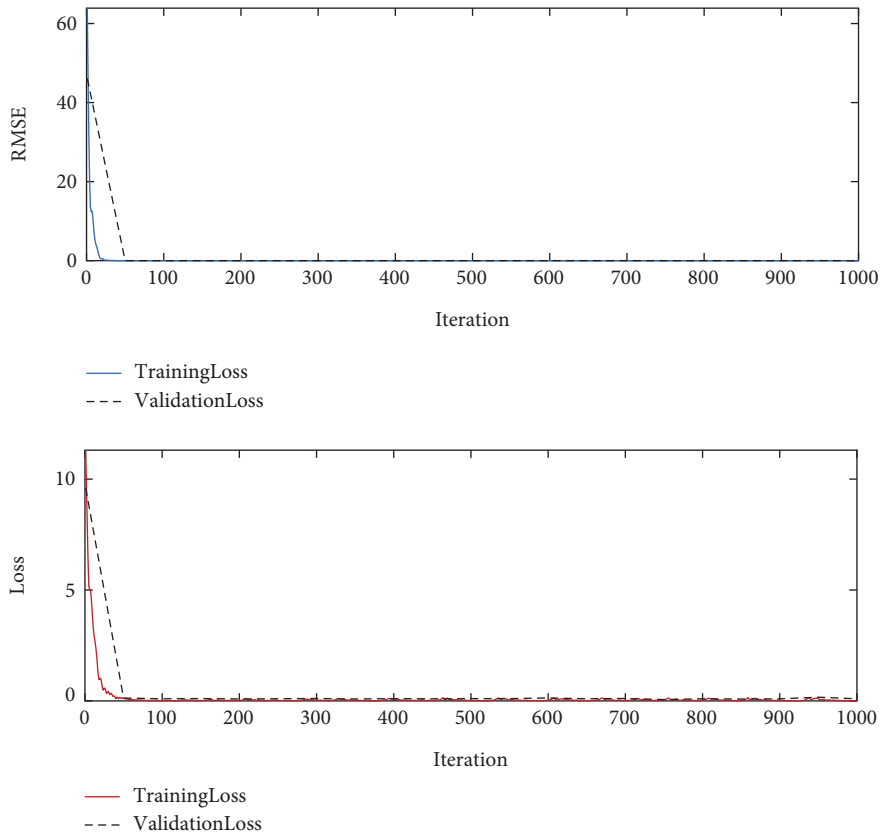

Figure 12: Pretraining effect of the source domain model by GRU.

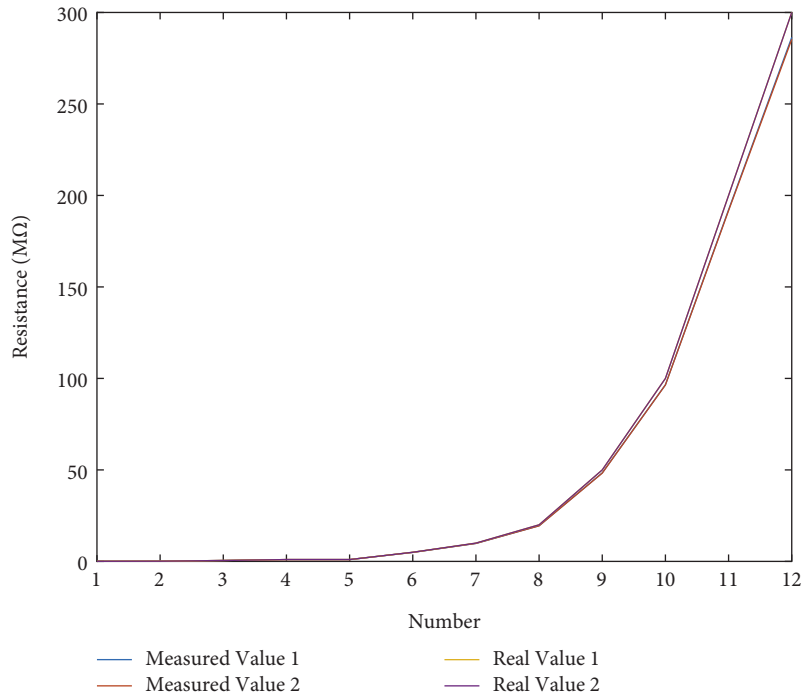

Figure 13: Measured values of insulation resistance.

3.4. Establishment of Transfer Learning Model. Transfer learning is a kind of machine learning approach, in which a pretrained model is reused in a task with another target model. The pretrained model is set as the source domain Ds, the training process of the pretrained model is the learning task Ts, the target model is set as the target domain Dt, and

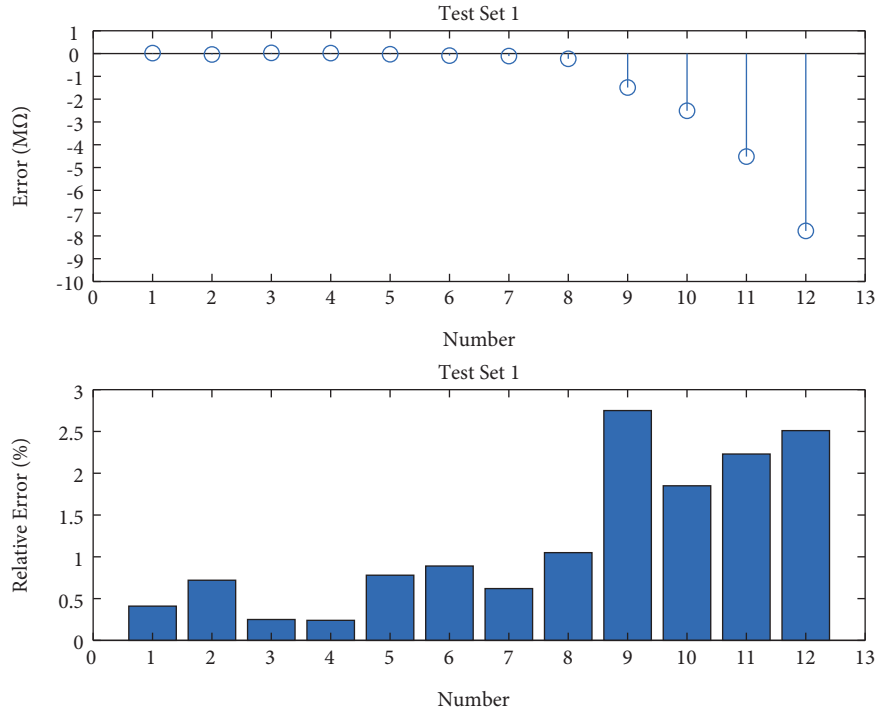

Figure 14: Diagram of insulation resistance measurement error and relative error in test set 1.

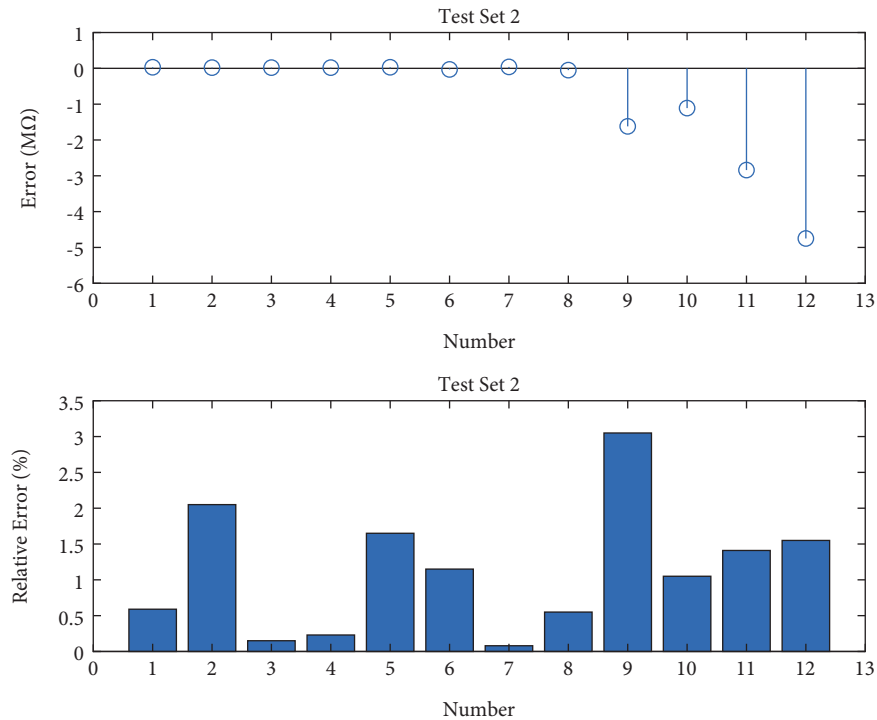

Figure 15: Diagram of insulation resistance measurement error and relative error in test set 2.

the training process of the target model is the learning task Tt . The source domain and the learning task are used to predict the rules of the target domain. It's worth noting that Ds ≠ Dt and Ts ≠ Tt .$D_T$and a learning task $T_T$on the target domain, $D_S$and$T_S$are used to learn the prediction function $f(\cdot)$ on the target domain and $D_S \neq D_T$ or $T_S \neq T_T$. Its core is to find the similarity or some mapping relationship between source domain D_S and target domain D_T [30, 31]. This paper adopts the parameter-based transfer learning method, and its basic idea is shown in Figure 16.

In the source domain, the LSTM model Net_S is trained with the source domain data, and the weight parameters of the lower

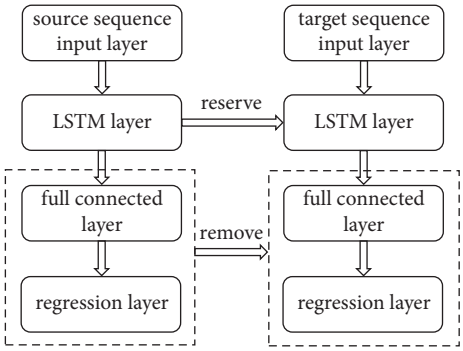

Figure 16: Schematic diagram of the parameter-based transfer learning idea.

layer of Net_S are fixed and applied to the LSTM model Net_T in the target domain. At the same time, the full connection layer and the regression layer of Net_T are rebuilt and the parameters are adjusted according to the input data of the target domain.

In this paper, the measurement of insulation resistance of the ANLS cable under low voltage condition is taken as the learning task in the source domain, and the measurement of insulation resistance of the ANLS cable under high voltage condition is taken as the learning task in the target domain. Resistance measurements at low voltage are relatively safe and readily available. The pretraining model is established after a lot of training, and the weight parameters of the pretraining model are applied to the target domain through the parameter-based transfer learning, which saves the training time and improves the measurement accuracy.

4. Measurement System Performance Analysis

4.1. Target Domain Data Acquisition. The purpose of transfer learning is to apply the model trained in advance to the target domain. In order to analyze the measurement performance of this design, an experimental platform of the ANLS is built. Figure 17 is a sinusoidal constant current dimmer, and Figure 18 is an ANLS circuit, which can be used to simulate high voltage conditions and actual working conditions (in addition to loop length).

In order to simulate the change of the ANLS circuit cable insulation resistance value, the target resistance B with known resistance value is made, as shown in Figure 19. It is connected in parallel to the cable of the light circuit, and different resistance values can be obtained by rotating the switch to simulate the change of insulation resistance.

Connect target resistance B to the "Target Plate" as shown in Figure 5. Place the device at room temperature and turn on the power. Then, turn on the switch of the target resistance B in Figure 19 and measure according to the steps in Section 2.2 to obtain a set of data. After cooling off the power and the equipment, measurements are made again after turning on the power and repeated for 6 times to form target domain data $\{R_{xt}, R_{yt}\}_1, \{R_{xt}, R_{yt}\}_2, \ldots, \{R_{xt}, R_{yt}\}_6$. The six sets of sequence data are divided into training set and test set according to 4 : 2.

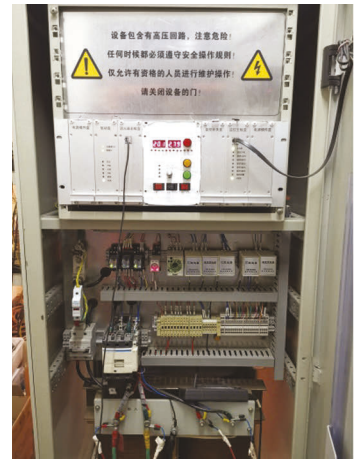

Figure 17: Sinusoidal constant current dimmer.

Figure 18: An ANLS circuit.

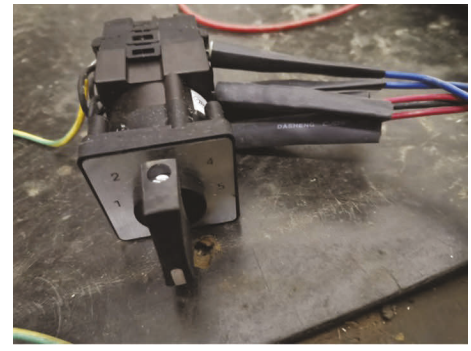

Figure 19: The target resistance B.

4.2. Target Domain Construction and Performance Analysis. Input the prepared target domain data into the model for training. The training results are shown in Figure 20, and the measurement results on test sets are shown in Figure 21.

Figure 21 shows the measurement results of insulation resistance values corresponding to the two test sets. The error of the measured value compared with the real value and the corresponding relative error are shown in Figures 22 and 23. As can be seen from Figures 21–23, the effect of the pretraining model is effective, and the relative error of the

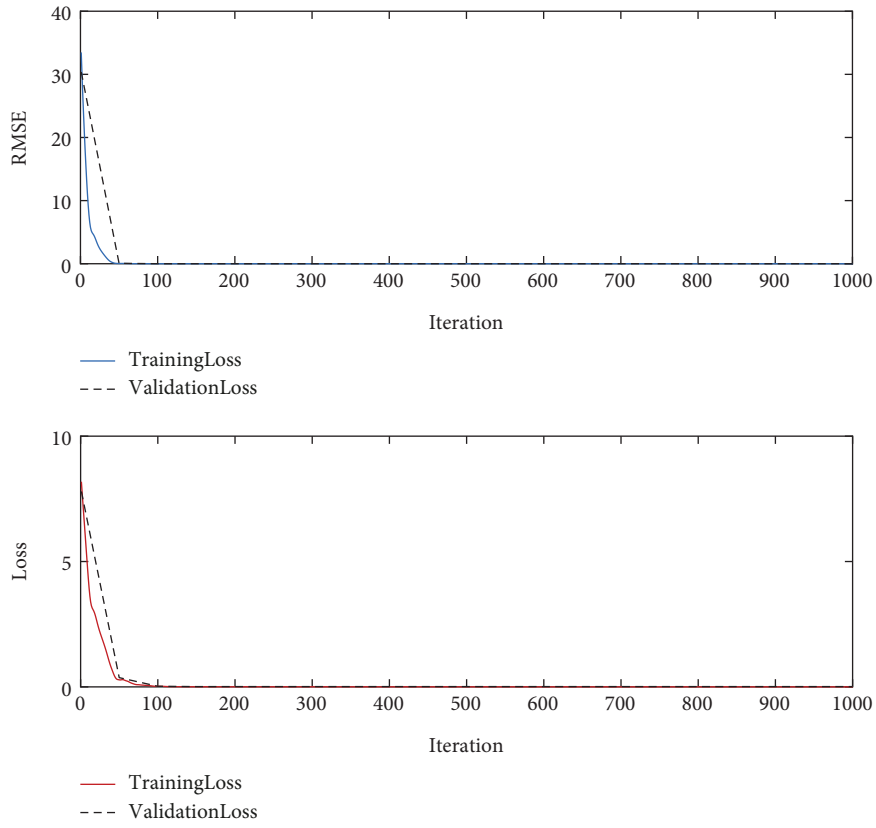

Figure 20: Model training results of target domain.

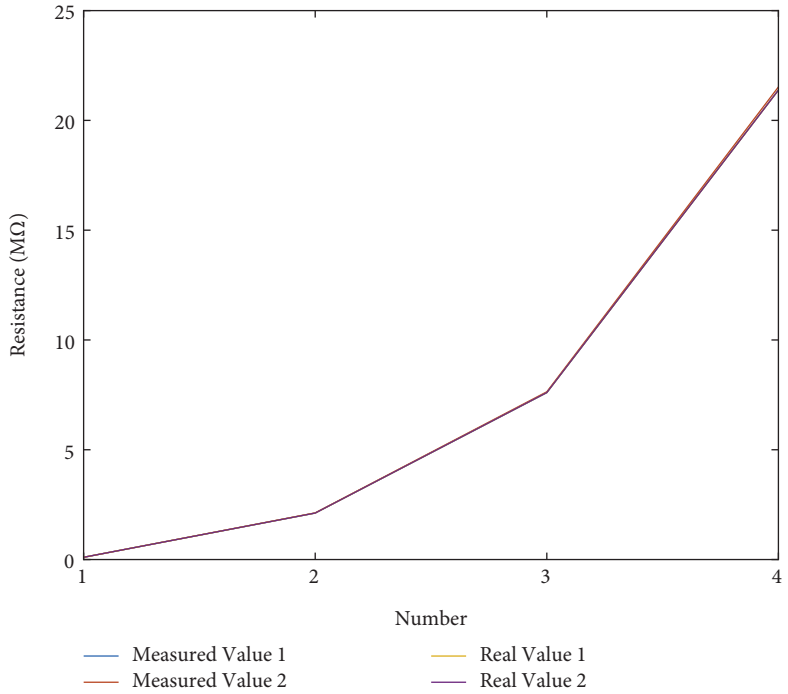

Figure 21: Measured values of insulation resistance.

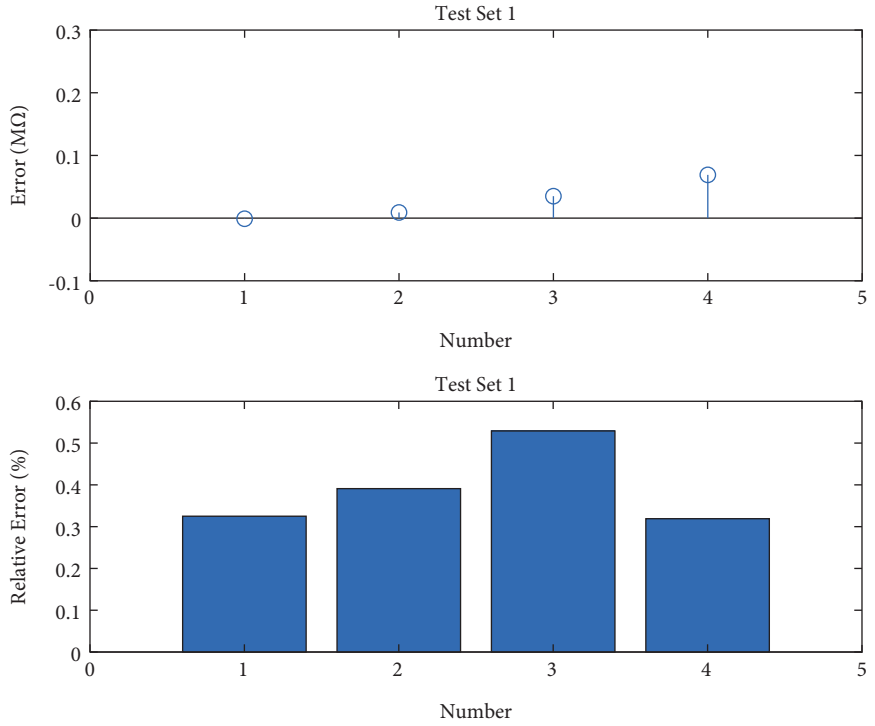

Figure 22: Diagram of insulation resistance measurement error and relative error in test set 1.

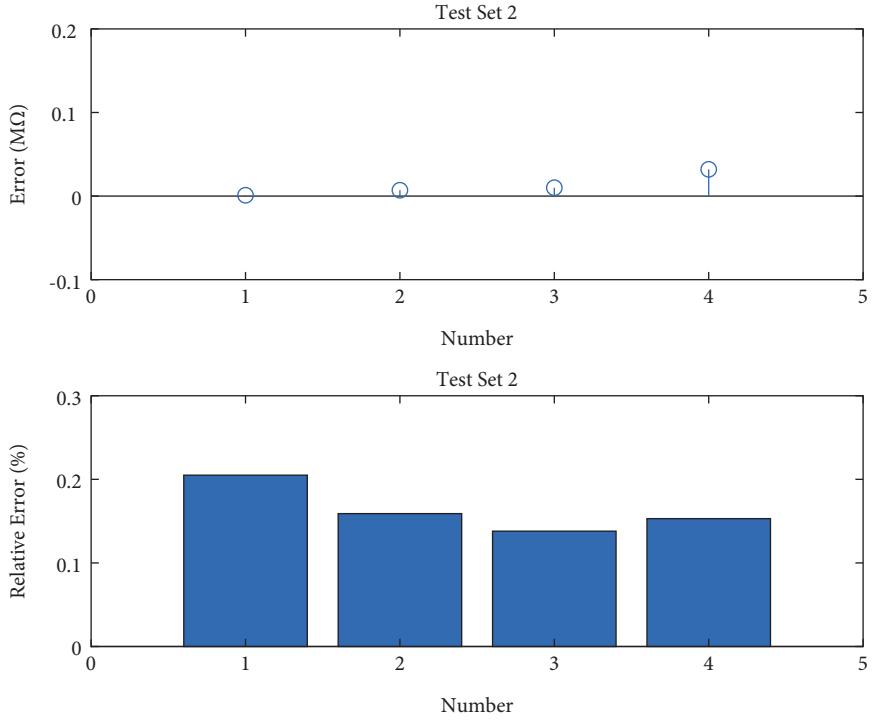

Figure 23: Diagram of insulation resistance measurement error and relative error in test set 2.

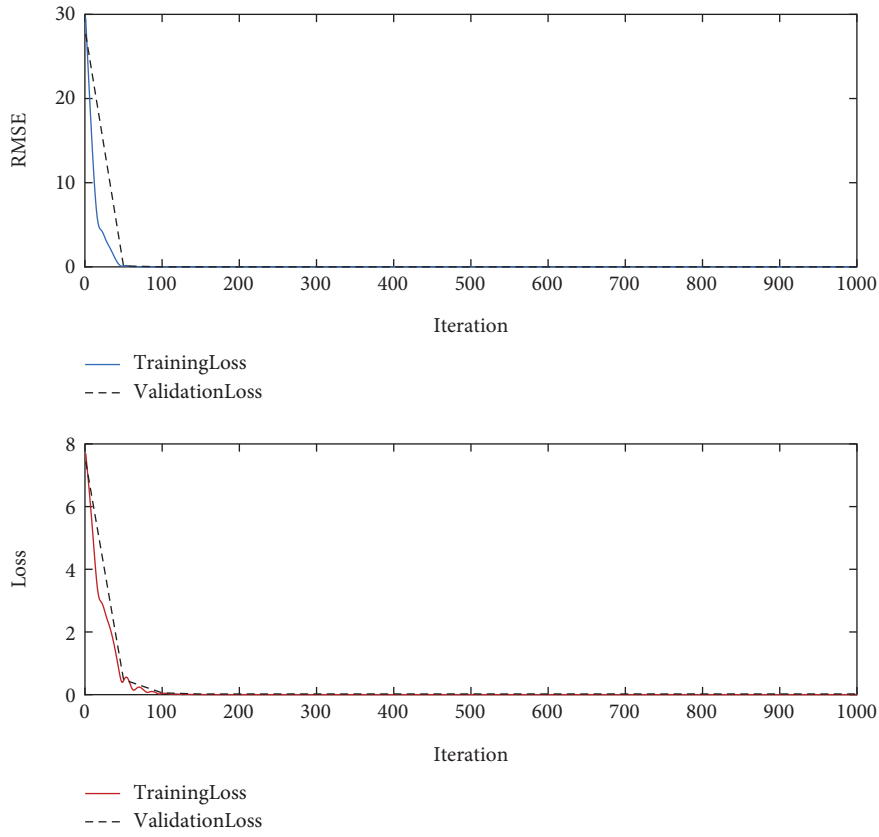

Figure 24: Training effect of the LSTM model without transfer learning.

insulation resistance value obtained on the test set can be controlled within 0.6%.

4.3. Overall Performance Comparison. In order to analyze the performance of the system, the insulation resistance of the ANLS circuit cable is tested by many ways. The target resistance B in Figure 14 is selected as the reference object. In this section, insulation resistance measurement results of three different methods, including switching time-sharing method, deep learning without transfer learning, and deep learning and transfer learning proposed in this paper, will be compared. Also, connect target resistance B to the "Target Plate" as shown in Figure 5. The change of insulation resistance value is simulated by rotating the switch under high voltage conditions for measurement.

Method 1 (switching time-sharing method). The insulation resistance value of the ANLS circuit cable is measured directly by the method in Section 2.2.

Method 2 (deep learning without transfer learning). Place the device at room temperature and turn on the power. Then, turn on the switch of the target resistance B in Figure 19 and measure according to the steps in Section 2.2 to obtain a set of data R_x. R_x is taken as the input data and the true value of the target resistance B is taken as the output data. The LSTM model in Figure 7 is used for training, and the model training result is shown in Figure 24. The model is directly applied to the measurement without subsequent transfer learning.

Table 1: Insulation resistance measurement results of the three methods.

True value of insulation resistance (MΩ)	Switching time-sharing method (MΩ)	Deep learning without transfer learning (MΩ)	Deep learning and transfer learning (MΩ)
0.1027	0.1040	0.1020	0.1025
2.1189	2.0943	2.1331	2.1222
7.6065	7.3363	7.6748	7.6173
21.3790	19.9578	21.5793	21.4121

Method 3 (deep learning and transfer learning). According to the method presented in this paper, the insulation resistance value is measured according to the steps in Section 3.1.

Results of the three measurement methods are shown in Table 1. To observe the measurement effect more intuitively, the insulation resistance values obtained by the three methods are compared and their relative errors are shown in Figure 25.

It can be seen from Figure 25 that the relative error of insulation resistance value obtained by the deep learning and transfer learning method is the smallest among the three measurement methods. When the insulation resistance value is small, the relative error of the three measurement

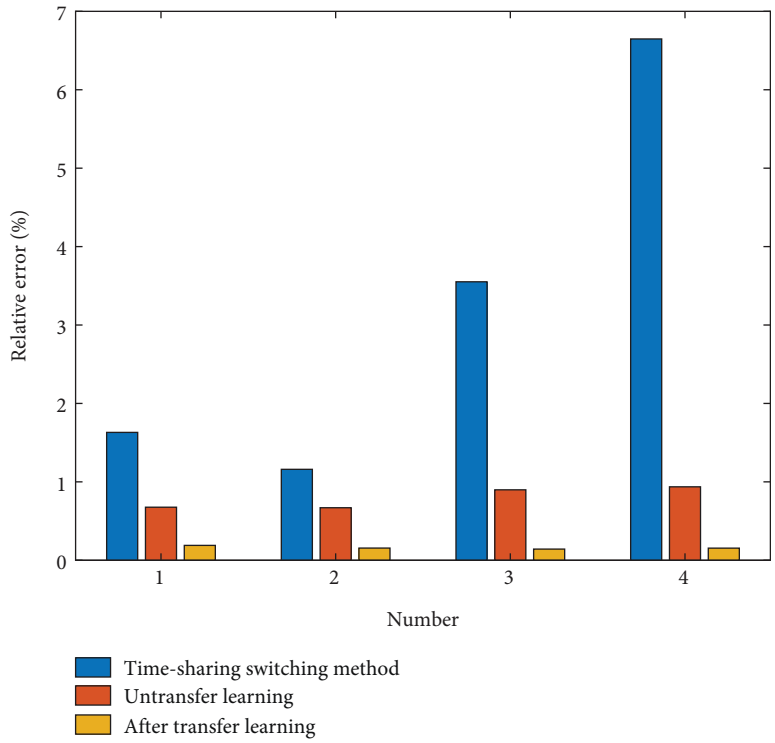

Figure 25: Relative error comparisons of insulation resistance values.

methods is relatively small. When the insulation resistance value of the cable to be measured increases, the measurement effect of the three methods becomes different. The switching time-sharing method has the largest relative error, while the deep learning and transfer learning method has the smallest relative error. The cable insulation resistance of the ANLS is generally extremely high under the actual working conditions. Therefore, the method proposed in this paper can improve the measurement accuracy of insulation resistance. Especially for high voltage and high insulation, the measurement effect is more stable. At the same time, the introduction of transfer learning can share the pretrained model parameters under low voltage conditions with the online measurement model under high voltage conditions, which saves the training time and increases the safety factor in the detection process and also solves the problem of small sample data. To sum up, the relative error of the deep learning and transfer learning method proposed in this paper is small and controlled within 0.6%, which indicates that this method can better reflect the real-time situation of the circuit cable insulation resistance and has a better indication effect on the current working state of the ANLS.

5. Conclusions

In this paper, deep learning and transfer learning are firstly applied in the measurement of insulation resistance in the ANLS. Aiming at reducing the influence of high voltage environment and voltage injection signal on the measurement accuracy of insulation resistance, a multilayer LSTM model is established, which is used for pretraining, and a normalized layer is added in front of the first LSTM layer to accelerate the data convergence rate. Then, based on the pretrained LSTM model, the weight parameter of the pretrained model is shared through transfer learning to solve the problem of small sample data. Simulation and experimental results show that the influence of the injection voltage signal and stray current on the measurement results is reduced. It has obvious advantages for the measurement of high insulation resistance value, and the relative error can reach less than 0.6%. Moreover, the measurement of insulation resistance value of the ANLS circuit cable has not formed an industry standard. The application of deep learning and transfer learning in this paper provides a new idea for the measurement method.

There are still new challenges: the weight of the pretrained model is shared for transfer learning in this paper, and the feature-based transfer learning method can be further considered. The data distribution under low pressure and high pressure conditions is mapped to the same feature space by establishing the joint distribution function of source domain data and target domain data to enhance domain adaptability.

Data Availability

The processed data used to support the findings of this study have not been made available because the data also form part of an ongoing study.

Conflicts of Interest

The authors declare that there are no conflicts of interest regarding the publication of this paper.

Acknowledgments

This work was supported in part by the Doctoral Research Start-up Foundation of Liaoning Province under Grant 2019-BS-040.

References

[1] N. K. Chawda, H. W. Schuett, and R. Wiechert, *Devices, Methods, and Systems for Alternating Current Circuits for Airfield Lighting*, Patent application 2018/0249540A1, U.S.A, 2018.

[2] Y. G. Yu, *Airfield Lighting Sustem. Patent Application 9131584B2*, U.S.A, 2015.

[3] J. Pablo Conti, "Airport of the future," *Engineering & Technology*, vol. 10, no. 1, pp. 66–68, 2015.

[4] T. Kurihara, E. Tsutsui, E. Nakanishi et al., "Investigation of water tree degradation in dry-cured and extruded three-layer (E-E Type) 6.6-kV removed XLPE cables," *Electrical Engineering in Japan*, vol. 198, no. 4, pp. 37–50, 2016.

[5] K. Steppe, "The potential of the tree water potential," *Tree Physiology*, vol. 38, no. 7, pp. 937–940, 2018.

[6] IEEE standard, *International Standard Norme International*, 2019.

[7] C. Zhang, C. Li, L. Nie, Z. Jing, and B. Han, "Research on the water blade electrode method for assessing water tree resistance of cross-linked polyethylene," *Polymer Testing*, vol. 50, pp. 235–240, 2016.

[8] P. Olszowiec, *Insulation Measurement and Supervision in Live AC and DC Unearthed Systems*, p. 15, Springer International Publishing, Berlin, 2014.

[9] R. Polansky and M. Polanská, "Testing of the fire-proof functionality of cable insulation under fire conditions via insulation resistance measurements," *Engineering Failure Analysis*, vol. 57, pp. 334–349, 2015.

[10] V. Verdingovas, S. Joshy, M. S. Jellesen, and R. Ambat, "Analysis of surface insulation resistance related failures in electronics by circuit simulation," *Circuit World*, vol. 43, no. 2, pp. 45–55, 2017.

[11] Y. Shen, A. Liu, and G. Cui, "Design of online detection system for insulation resistance of electric vehicle based on unbalanced bridge," in *Proceedings of the 2019 IEEE Innovative Smart Grid Technologies-Asia (ISGT Asia)*, pp. 537–542, IEEE, Chengdu, China, May 2019.

[12] Y. H. Chiang, W. Y. Sean, C. Y. Huang, and L. H. Chiang Hsieh, "Adaptive control for estimating insulation resistance of high-voltage battery system in electric vehicles," *Environmental Progress & Sustainable Energy*, vol. 36, no. 6, pp. 1882–1887, 2017.

[13] X. Jian and G. Hong, "An intelligent dual-voltage driving method and circuit for a common rail injector of heavy-duty diesel engine," *IEEE Access*, vol. 5, pp. 27681–27689, 2017.

[14] C. Song, Y. Shao, S. Song et al., "Insulation resistance monitoring algorithm for battery pack in electric vehicle based on extended Kalman filtering," *Energies*, vol. 10, no. 5, p. 714, 2017.

[15] N. Shtabel, L. Samotik, and E. Mizrakh, "Fluxgate direct current sensor for real-time insulation resistance monitoring," in *Proceedings of the 2019 International Conference on Industrial Engineering, Applications and Manufacturing (ICIEAM)*, Sochi, Russia, March 2019.

[16] X. Jian and G. Hong, "An online adaptive monitoring system for insulation resistance of electric vehicles," in *Proceedings of the 2019 IEEE 2nd International Conference on Information Systems and Computer Aided Education (ICISCAE)*, pp. 37–41, Dalian, China, September 2019.

[17] S. Hao, X. Zhang, R. Ma, and G. Jie, "Fault line selection method for small current grounding system based on improved GoogLeNet," *Power System Technology*, vol. 2021, pp. 1–9, Article ID 678120, 2021.

[18] Y. Li, Y. Wang, Y. Zhang, and J Zhang, "Diagnosis of interturn short circuit of permanent magnet synchronous motor based on deep learning and small fault samples," *Neurocomputing*, vol. 442, pp. 348–358, 2021.

[19] T. J. Donnelly and S. D. Pekarek, "Modeling and control of an LED-based airfield lighting system," in *Proceedings of the IEEE Power and Energy Conference at Illinois (PECI)*, pp. 1–5, Champaign, IL, USA, April 2018.

[20] I. V. Komlev and Komlev, "On associated data and power channels in the cable ring of an airfield lighting system," *Russian Electrical Engineering*, vol. 90, no. 5, pp. 412–416, 2019.

[21] X. Ma, T. Li, J. Li, and F. Chen, "Airport-specific light-guiding taxiing guidance sign," in *Proceedings of the 2020 IEEE 3rd International Conference on Electronics Technology (ICET)*, pp. 207–2111, Chengdu, China, May 2020.

[22] Y. Yan, S. D. Sudhoff, J. Nadel, and D. W. Gallagher, "Modeling and stability analysis of a fixture-centric airfield lighting System," *IEEE Transactions on Aerospace and Electronic Systems*, vol. 55, no. 6, pp. 3479–3491, 2019.

[23] M. Liu, "Design of airport navigation aid lighting system based on LED," *International journal of science*, vol. 5, pp. 102–105, 2018.

[24] Y. Zhang, *The Design and Implementation for Real-Time Online Monitoring Unit of Insulation Resistance in Airfield Lighting Circuit*, M. S. thesis, Dalian Jiaotong University, Dalian China, 2015.

[25] S. Li, X. You, and S. Liu, "Multiple ant colony optimization using both novel LSTM network and adaptive Tanimoto communication strategy," *Applied Intelligence*, vol. 51, no. 8, pp. 5644–5664, 2021.

[26] X. Wu, Z. Du, Y. Guo, and H. Fujita, "Hierarchical attention based long short-term memory for Chinese lyric generation," *Applied Intelligence*, vol. 49, no. 1, pp. 44–52, 2019.

[27] T. Bogaerts, A. D. Masegosa, J. S. Angarita-Zapata, E. Onieva, and P. Hellinckx, "A graph cnn-lstm neural network for short and long-term traffic forecasting based on trajectory data," *Transportation Research Part C: Emerging Technologies*, vol. 112, pp. 62–77, 2020.

[28] Y. Zhang, Y. Xin, Z. Liu, and M. Guijun, "Health Status Assessment and Remaining Useful Life Prediction of Aero-Engine Based on BiGRU and MMoE," *Reliability Engineering & System Safety*, vol. 220, 2022.

[29] A. Flores, H. Tito-Chura, and V. Yana-Mamani, "An ensemble GRU approach for wind speed forecasting with data augmentation," *International Journal of Advanced Computer Science and Applications*, vol. 12, no. 6, pp. 569–574, 2021.

[30] S. J. Pan and Q. Yang, "A survey on transfer learning," *IEEE Transactions on Knowledge and Data Engineering*, vol. 22, no. 10, pp. 1345–1359, 2010.

[31] M. Wang and W. Deng, "Deep visual domain adaptation: a survey," *Neurocomputing*, vol. 312, pp. 135–153, 2018.